SSVEP-Based Brain-Computer Interface for Cursor Control

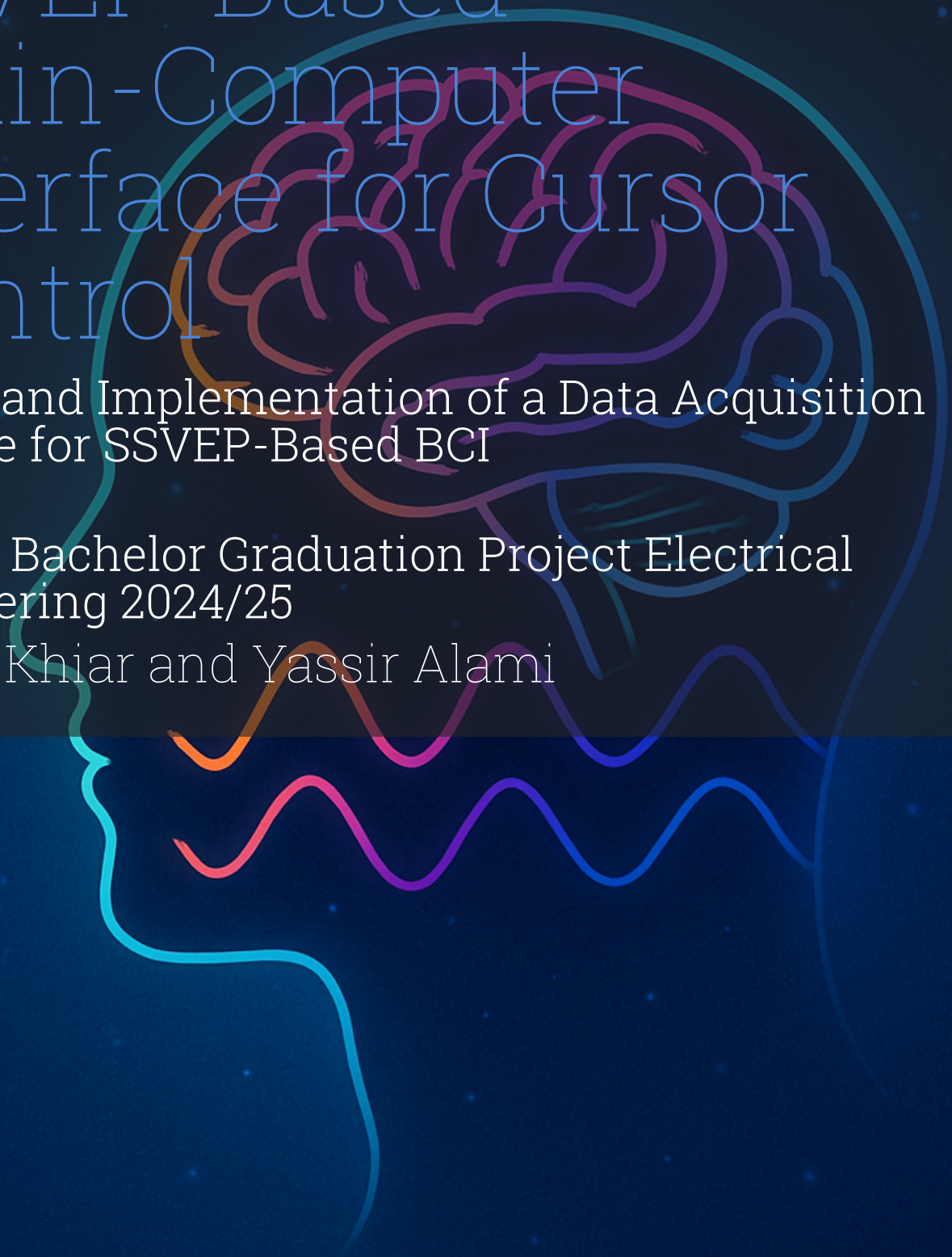

Design and Implementation of a Data Acquisition Pipeline for SSVEP-Based BCI

EE3L11: Bachelor Graduation Project Electrical Engineering 2024/25

Wissal Khiar and Yassir Alami

Delft University of Technology

TU Delft

SSVEP-Based Brain-Computer Interface for Cursor Control

Design and Implementation of a Data Acquisition Pipeline for SSVEP-Based BCI

by

Wissal Khiar and Yassir Alami

Student Name	Student Number
Wissal Khiar	5786622
Yassir Alami	5842344

Supervisors: Tiago Costa and Dante Muratore
Project Duration: April, 2025 - June, 2025
Faculty: Faculty Electrical Engineering, Mathematics and Computer Science, Delft

TU Delft

Preface

Wissal Khiar and Yassir Alami
Delft, June 2025

This paper marks the completion of our Bachelor's graduation project, conducted as part of a collaborative effort to develop a real-time Brain-Computer Interface (BCI) system. The project was carried out by three dedicated groups: GUI and Stimulus Design, Signal Acquisition, and Signal Processing and Classification. Our group was responsible for the second, focusing on reliably capturing and delivering clean EEG signals from the Unicorn Hybrid Black headset for further processing and classification.

Working on this project has been both challenging and rewarding. It provided us with the opportunity to apply and expand our knowledge in biomedical signal acquisition, while also learning how to collaborate effectively within a multidisciplinary team. The experience gave us valuable insights into the practical challenges of recording high-quality brain signals in real time and the importance of precise measurement setups in the success of BCI systems.

We would like to sincerely thank our supervisors, Tiago Costa and Dante Muratore, for their ongoing support, guidance, and constructive feedback throughout the course of the project. Their expertise and encouragement played a crucial role in helping us stay motivated and on track.

We hope this work will contribute to further developments in the field of BCI, and we are excited to see how future students and researchers will build upon it.

Abstract

This project explores the development of a real-time Brain-Computer Interface (BCI) system based on Steady-State Visually Evoked Potentials (SSVEPs). The aim is to enable hands-free computer control by detecting brain responses to visual stimuli flickering at specific frequencies. Our focus was on the acquisition of clean and stable EEG signals using the Unicorn Hybrid Black headset. Key challenges included minimizing noise from motion and eye artifacts, selecting the right channels for SSVEP detection, and applying appropriate filters. While the hardware setup and real-time streaming via Lab Streaming Layer (LSL) were successfully established, consistent frequency detection during visual stimulus trials remains an unresolved issue. Controlled tests with simulated signals confirmed that the pipeline can detect known inputs, indicating that future work should focus on improving artifact removal and stimulus reliability. The current system provides a solid foundation for further development toward robust, real-time brain-controlled interfaces

Contents

1 Introduction

1.1. State-of-the-Art Analysis

Brain-Computer Interfaces (BCIs) are systems that enable direct communication between the brain and an external device by translating neural activity into actionable commands, bypassing peripheral nerves or muscular control [1]. Non-invasive BCI systems, particularly those based on electroencephalography (EEG), are very attractive due to their safety, portability, and relatively low cost [2]. BCIs have shown promise in restoring communication or control abilities to individuals with severe motor impairments. In recent years, however, BCI applications have extended into broader domains including entertainment, neurofeedback training, and assistive technologies for the general population [3], [4].

Among various BCI paradigms, the Steady-State Visual Evoked Potential (SSVEP) approach stands out for its robustness, minimal training requirements, and high information transfer rates. SSVEPs are brain responses elicited when a user focuses on a visual stimulus flickering at a constant frequency, making this paradigm particularly suitable for real-time applications [5]. Thanks to advances in signal processing and machine learning, modern SSVEP-based BCIs now achieve significantly improved accuracy and responsiveness, bringing real-time control applications closer to practical deployment [6]. However, achieving seamless integration between signal acquisition, real-time processing, and graphical interface design remains a key technical challenge [7].

1.2. Problem Definition

For this project a real-time SSVEP BCI is being developed that moves a computer cursor. The data-acquisition subgroup must deliver a continuous, low-latency EEG stream that preserves SSVEP information while operating with:

- Fixed hardware: The eight-channel Unicorn Hybrid Black with dry electrodes is predetermined, limiting electrode placement and access to raw firmware settings.
- Real-world conditions: Recordings must remain usable when users blink, shift slightly, or when environmental electromagnetic noise is present.
- Live processing needs: Data have to be time-synchronized (via Lab Streaming Layer) so that stimulus presentation, filtering, and classification run in their usual procedure.

If clean, stable signals cannot be guaranteed, downstream modules—stimulus design and classification—cannot reach the accuracy required for reliable cursor control. The core challenge is therefore to refine the measurement setup, optimise electrode contact, apply on-the-fly noise suppression, and stream the data with minimal delay.

1.3. Thesis Synopsis

This thesis documents the work of the data acquisition subgroup in setting up a reliable EEG measurement system for an SSVEP-based BCI. The report begins with a specification of the programme of requirements, defining the key performance and technical targets for the system. Next, the measurement setup is described in detail, including hardware use, electrode positioning, and testing conditions. Following that, the filtering and artifact removal strategies are presented to show how signal quality was improved in real time. The results chapter then evaluates the effectiveness of the setup based on both controlled signal injections and actual recordings. Finally, the report concludes with a discussion on system performance, encountered limitations, and recommendations for future improvements.

2

System Overview

This section presents a high-level overview of the SSVEP-based BCI system developed in this project. It describes the overall system architecture, including its core subsystems and their interactions, and clarifies the role of the Data Acquisition sub-group within the larger system. The objective is to establish a clear conceptual understanding of the system's structure and data flow before addressing implementation details and integration strategies in later chapters.

2.1. Overall System Architecture

The BCI system is composed of three main subsystems: Graphical User Interface (GUI), Data Acquisition, and Signal Processing. These components form an integrated loop that enables both various EEG-driven functionalities and real-time cursor control.

As illustrated in Figure 2.1, the pipeline begins with the GUI, which initiates a connection to the EEG headset using the Lab Streaming Layer (LSL) protocol. LSL is an open-source framework designed for real-time collection, transmission, and synchronization of EEG data from devices such as the Unicorn Hybrid Black headset and other biosignal devices. Once the stream is active, the headset continuously transmits raw EEG data. This data is utilized by the GUI in multiple contexts, such as live EEG visualization or during configurable recording trials for data collection.

In parallel, the streamed EEG data is forwarded to the backend pipeline responsible for real-time control. This begins with the Data Acquisition subsystem, which applies pre-processing techniques including filtering and artifact removal. The cleaned EEG data is then passed to the Signal Processing subsystem, where classification is performed to determine the user's intended action by detecting SSVEP responses associated with specific visual stimuli. The resulting classification output, consisting of the predicted frequency and a confidence score, is returned to the GUI, which translates this output into interactive feedback, including cursor movement and on-screen visual indicators.

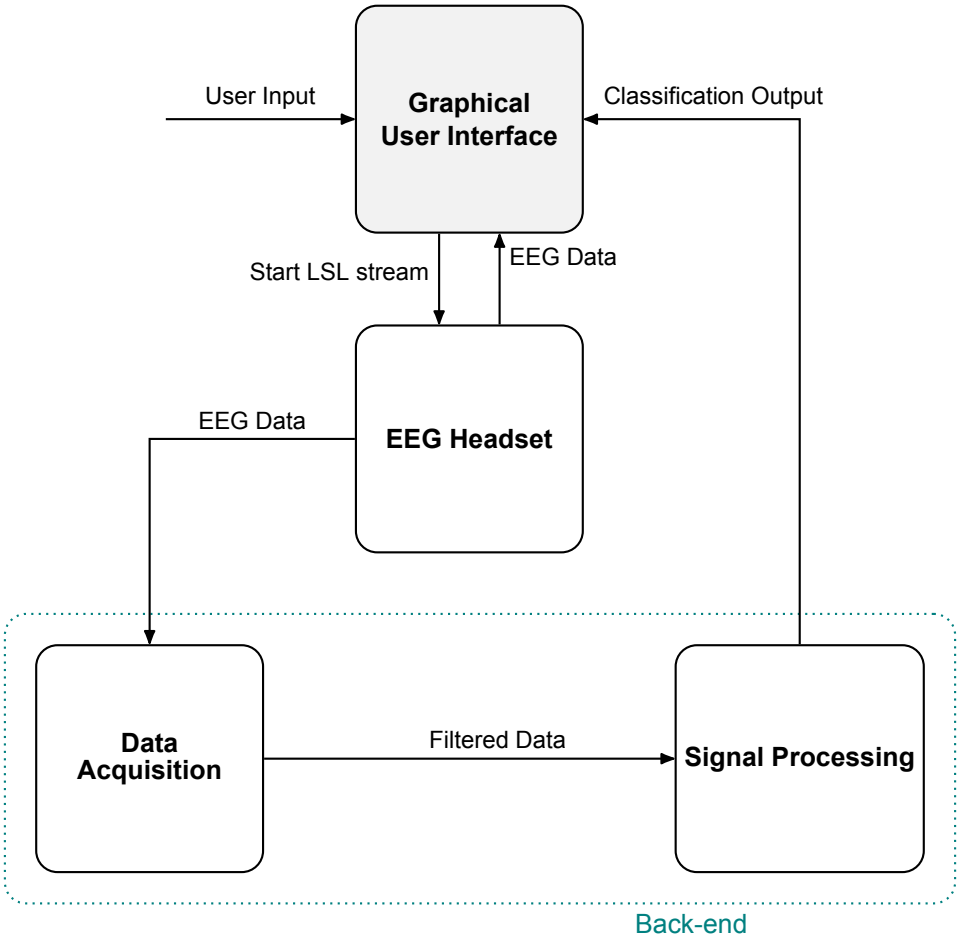

Figure 2.1: Overall System Architecture

2.2. Role of Data Acquisition Subgroup

The data acquisition subgroup was tasked with setting up a reliable system to record brain signals in real time. The EEG headset used—Unicorn Hybrid Black—had already been provided at the start of the project, so no hardware selection was required.

Care was taken to ensure the headset was fitted properly and that the electrodes made solid contact with the scalp. Various methods were tested to improve signal quality, including careful positioning and the use of conductive gel to reduce interference caused by small movements or external disturbances.

The subgroup was also responsible for making sure that the recorded brain signals could be streamed live to the other parts of the system, allowing real-time collaboration with the stimulus presentation and classification components.

In summary, the role of the data acquisition subgroup was to ensure that high-quality EEG signals were captured and made available for further processing by the other subsystems.

3

Programme of Requirements

The following key requirements were defined for the signal acquisition subsystem of the BCI:

- Dry Electrode EEG Acquisition: Use the Unicorn Hybrid Black headset to record EEG signals from the scalp using dry electrodes. The system must capture brain signals relevant to SSVEP while maintaining user comfort and safety.
- Targeted Channel Selection: Focus on electrode locations over the visual cortex (occipital region) to maximize SSVEP signal strength. In particular, utilize the headset channels corresponding to occipital and parietal-occipital sites for SSVEP detection, while also monitoring a frontal channel for artifacts.
- Noise and Artifact Minimization: Ensure that the acquired signals have a high signal-to-noise ratio by minimizing common EEG noise sources. The hardware and software design should mitigate power-line interference (50 Hz mains noise), environmental electromagnetic disturbances, and movement artifacts. Physiological artifacts such as eye-blinks and muscle activity should be actively monitored and filtered out to prevent contamination of the SSVEP signals.
- Filtering and Preprocessing Pipeline: Implement a preprocessing pipeline that conditions the raw EEG signals for analysis. This includes removal of DC offsets and slow drifts, bandpass filtering to isolate the frequency range of interest for SSVEP (while preserving relevant harmonics), and notch filtering to suppress line noise. All filtering stages should be designed to introduce minimal distortion or delay, preserving the integrity of genuine SSVEP features.
- Reliability under Real-World Conditions: The acquisition setup should be robust against typical real-world conditions. It must maintain signal quality over the course of an experiment, accounting for factors like slight headset shifts, varying impedance at the electrode-skin interface, and external distractions. The system should produce stable and repeatable results without requiring excessive recalibration or user intervention during operation.
- Integration for Cursor Control: Deliver sufficiently clean and discriminative EEG signals to enable the detection of user intent via SSVEP frequency recognition. The end-to-end performance of the acquisition system should support the overall goal of controlling a computer cursor, meaning the captured signals must allow the classification subsystem to reliably distinguish different visual stimulus frequencies corresponding to control commands.

4

Measurement setup

To obtain reliable EEG signals from the brain, careful attention was given to the setup of the measurement system. As these signals are inherently weak and highly sensitive to noise and movement, this chapter outlines how the measurement setup was constructed, evaluated, and refined through systematic testing.

4.1. Brain Patterns

Certain parts of the brain can be used to detect electrical activity linked to specific functions. In the case of visual stimulation, activity is mainly generated in the visual cortex, which is located in the occipital lobe at the back of the head. When a person focuses on a flickering visual stimulus, the brain produces signals known as Steady-State Visual Evoked Potentials (SSVEPs).

These signals are strongest in the occipital and parietal-occipital regions, which is why electrodes placed in those areas are commonly used for SSVEP-based Brain-Computer Interfaces. This study [8] shows that the strength and clarity of SSVEP responses depend heavily on electrode placement in the visual areas of the brain

4.2. Electrode Placement and Brain Regions

The Unicorn Hybrid Black is a non-invasive EEG headset that records brain activity through scalp electrodes. Internally, the Unicorn headset amplifies and digitizes the EEG signals at a sampling rate of 250 Hz with 24-bit resolution. The device communicates wirelessly to a computer via Bluetooth. It uses dry electrodes that make contact with the scalp to pick up tiny voltage differences caused by neuronal activity. To record these signals, two additional electrodes are placed on the mastoid area (behind the ears) serving as the reference. Once the headset is properly positioned, each electrode is adjusted (by slight twisting or pressing through hair) to ensure it contacts the scalp securely. In some cases, a small amount of gel was applied to each electrode to improve conductivity. Good electrode-skin contact lowers the impedance and significantly improves signal quality, making the system less sensitive to small movement

The Unicorn Hybrid Black headset is equipped with a fixed number of electrodes in predefined positions (shown in Figure 2.1) . Based on previous research, channels 6, 7, and 8 were selected as the primary focus for SSVEP signal acquisition [8] [9]. These channels correspond to the occipital and parietal-occipital regions of the brain, which are responsible for visual processing (shown in Figure 2.2). Since SSVEP responses originate in the visual cortex when a flickering stimulus is observed, these channels are considered the most effective for detecting such activity.

Channel 1, located near the frontal region, was monitored for eye-blink artifacts. Although not used for SSVEP detection, it serves as a useful reference channel for identifying and mitigating signal artifacts caused by blinking or facial movements. A more detailed discussion of artifact removal can be found in Section 4.3, Artifact Removal.

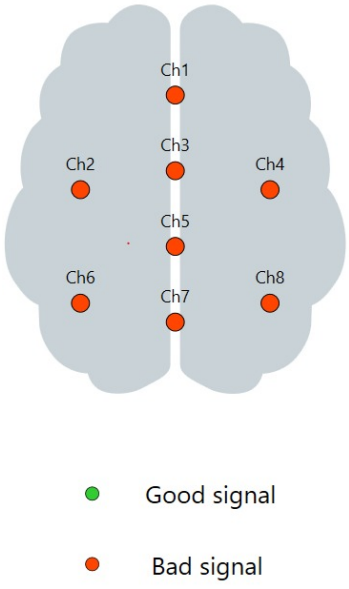

Figure 4.1: Channels on the Unicorn Hybrid Black headset

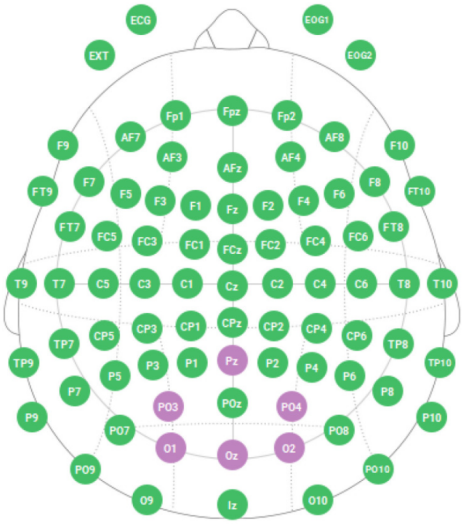

Figure 4.2: Top view of the standard 10–20 EEG layout, highlighting occipital and parietal-occipital electrode sites (in purple) typically used for SSVEP recordings. The visual cortex is located beneath the occipital scalp region, so electrodes placed here capture the strongest SSVEP signals [8].

4.3. EEG Data Collection: Recorder vs GUI

Two tools were used for collecting EEG data: the Unicorn Recorder and a custom-built GUI. The Unicorn Recorder, provided by the headset manufacturer, was initially used to check signal quality. Once all channels showed stable, low-noise readings, data collection could begin.

For the main experiments, a custom GUI was used instead. This setup allowed real-time EEG plots via LSL-streaming. The Lab Streaming Layer (LSL) is a tool that sends data from one program to another in real time, making it useful for live EEG recordings. Unlike the Unicorn Recorder, which required manual start/stop actions for each trial, the GUI automated the process—presenting stimuli and recording everything in sync.

Additionally, the GUI offered clearer and more organized signal plots. Instead of eight signals stacked vertically, it displayed them in two columns of four, allowing for higher resolution and easier monitoring. The GUI also included labeled axes (e.g., voltage in µV), which the Unicorn Recorder did not provide

This made the setup more efficient and user-friendly. Real-time measurements became possible, trials ran automatically, and the data could be accessed and processed in real time—all things the Unicorn Recorder did not support.

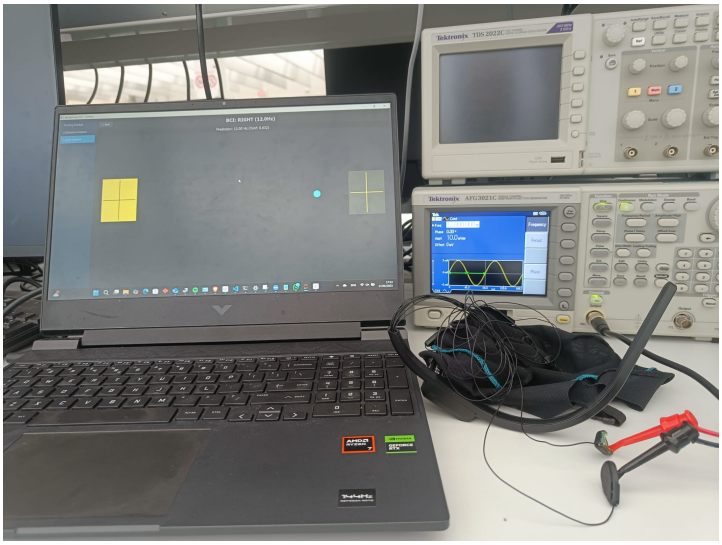

Figure 4.3: The custom-built GUI

4.4. Practical Testing and Setup Refinement

Once the initial setup was in place, several practical steps were taken to improve the stability and reliability of the EEG recordings. Testing was done under controlled conditions to identify and reduce sources of noise and signal loss.

The participant was seated at a fixed distance from the stimulus screen in a quiet environment with minimal background movement and distractions. This helped limit external interference during data collection. The headset was tightly secured to reduce shifts during trials, and electrode contact was carefully adjusted for each participant to ensure consistent readings.

To further improve signal stability, saline gel was applied to all electrodes. This helped reduce impedance and made the system less sensitive to small movements, especially around the hairline. Small adjustments in posture and screen distance were also tested to optimize user comfort while maintaining signal quality.

The recordings were only started when the signal was visibly stable across all channels. In between trials, short breaks were included to keep the participant focused and avoid fatigue-related artifacts. Through this process of repeated testing and refinement, a consistent and repeatable setup was developed for use in later experiments.

5

Filtering

Filtering is a critical step in EEG signal processing. EEG signals are inherently prone to various artifacts, classified broadly into physiological and non-physiological artifacts. The presence of these artifacts significantly impacts the performance of Brain-Computer Interfaces (BCIs), reducing accuracy and complicating user intention detection. Effective filtering methods are therefore necessary to mitigate these issues and ensure robust and precise BCI operation.

5.1. Background and Theoretical Foundation

5.1.1. Types of EEG Noise and Artifacts

In BCI applications, physiological artifacts originate from the user's biological activities, prominently including muscle contractions, eye blinks, and cardiac rhythms. Muscle artifacts (EMG) introduce high-frequency noise into EEG data, complicating signal analysis and accurate intention detection. Eye blinks and movements (EOG) produce distinctive low-frequency distortions, particularly affecting frontal electrode signals, while cardiac signals (ECG) may interfere primarily in lower frequency bands, potentially obscuring relevant EEG components.

Non-physiological artifacts arise from external sources such as equipment interference and electrical line noise, notably at 50 Hz. Line noise commonly occurs due to power supply interference, producing persistent artifacts that significantly degrade the quality of the EEG signal. Furthermore, electromagnetic interference from EEG hardware, cables, or nearby electronic devices introduces unpredictable distortions. Addressing these artifacts through careful hardware setup and targeted filtering techniques is crucial for maintaining the reliability and accuracy of BCI systems.

5.1.2. Butterworth Filter

The Butterworth filter, an Infinite Impulse Response (IIR) design, is characterized by its maximally flat magnitude response within the passband. Its squared magnitude response is given by:

$$|H(\omega)|^2 = \frac{1}{1 + \left(\frac{\omega}{\omega_c}\right)^{2n}}, \tag{5.1}$$

where ω_c denotes the cutoff frequency and n specifies the filter order. In EEG–BCI preprocessing, a zero-phase implementation is preferred: the filter is applied forward and then backward (e.g., via the `filtfilt` function) to eliminate phase shifts. This approach preserves the amplitude of SSVEP components while effectively attenuating noise outside the desired frequency band.

5.1.3. Signal-to-Noise Ratio in SSVEP

Welch power–spectral density

Before any SNR is calculated, EEG power is estimated with the Welch PSD. Welch's method splits each epoch into overlapping segments, applies windowing, computes a periodogram for every segment, and then averages those periodograms. Averaging lowers the variance of single-segment FFTs, while windowing limits spectral leakage. For the present data a 2s window with 50 % overlap was used, giving a frequency resolution of $\Delta f = 0.2$ Hz. This resolves the 8.57 Hz and 12 Hz targets yet leaves enough segments for a stable average. The resulting spectrum $P(f)$ is therefore smoother and more reliable than a raw FFT and is used in both SNR definitions below.

Time-domain SNR

Time-domain SNR in SSVEP experiments is defined by comparing the signal power during stimulation against a separate baseline (no-stimulus) period. One computes the power spectral density (PSD) of the EEG during stimulation and during baseline, then takes their ratio:

$$\mathrm{SNR}_{\mathrm{time}} = \frac{P_{\mathrm{stim}}(f_0)}{P_{\mathrm{base}}(f_0)}. \tag{5.2}$$

For instance, if the EEG shows a spectral peak at the stimulus frequency during flicker, this peak's power is divided by the power at the same frequency in the baseline recording [10].

Frequency-domain SNR

Frequency-domain SNR leverages the narrowband nature of SSVEP responses by estimating noise from neighboring frequency bins within the same trial. If $P(f_0)$ is the power at the target stimulation frequency f_0, and P_{noise} the average power of adjacent bins (excluding f_0), then

$$\mathrm{SNR}_{\mathrm{freq}} = \frac{P(f_0)}{P_{\mathrm{noise}}}. \tag{5.3}$$

often expressed in decibels as $10 \log_{10}[P(f_0)/P_{\mathrm{noise}}]$. An SNR > 1 indicates a clear spectral peak above the local noise floor.

5.1.4. Fast Fourier Transform for Signal Validation

To validate the integrity of our recorded EEG data prior to classification, we apply the Fast Fourier Transform (FFT) to each epoch. The FFT converts a time-domain signal $x[n]$ of length N into its discrete frequency components:

$$X[k] = \sum_{n=0}^{N-1} x[n]\, e^{-i2\pi nk/N} \tag{5.4}$$

where k corresponds to frequency $f_k = k\,(F_s/N)$ and F_s is the sampling rate. By choosing N so that each stimulation frequency aligns exactly with an FFT bin (i.e. an integer number of cycles per epoch), we maximize resolution at those frequencies.

From the complex spectrum $X[k]$, we compute the magnitude $|X[k]|$ or power $|X[k]|^2$. SSVEP responses appear as pronounced peaks at tag frequencies in the power spectrum. We therefore inspect power at each expected stimulation frequency across occipital channels, averaging over electrodes and epochs. Clear, high-amplitude peaks (or elevated SNR) confirm that our EEG acquisition captured the expected neural responses with sufficient fidelity. These FFT-derived spectral features serve as both a quality check and inputs for subsequent classification analyses.

5.2. Preprocessing

The preprocessing stage can be split in 4 stages as can be seen in the following flowchart.

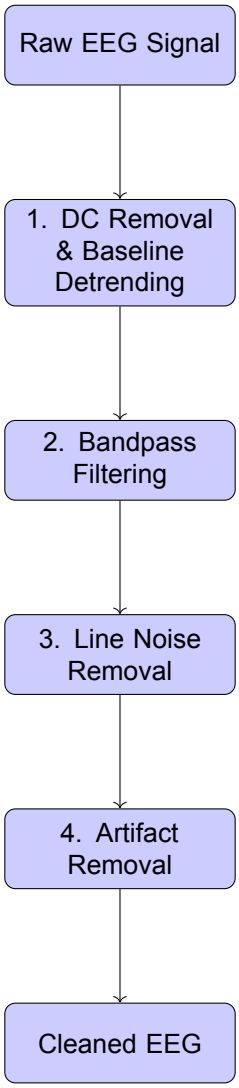

5.2.1. DC removal and Baseline Detrending

DC removal eliminates constant voltage offsets to center signals around zero, while baseline detrending removes slow, non-linear drifts caused by artifacts like sensor instability or movement, ensuring clean and interpretable data for downstream analysis. A 4th order butterworth high pass filter with a cutoff frequency of 0.5 Hz is sufficient to tackle this [11].

5.2.2. Filtering frequency ranges for SSVEP

Another study [12] suggests using a filter range of 0.5 to 50 Hz because this range includes most of the energy of the brain signal. A major benefit of this approach is that the 0.5 Hz lower limit automatically removes DC shifts and reduces slow drifts in the data, which results in not having to use the filter as mentioned in 5.2.1.

The frequency range that is ultimately used is 5 - 45Hz. This range was chosen, because it includes the SSVEP range and their harmonics which are used for classifying.

5.2.3. Line noise removal

Line noise (also called power-line interference) refers to unwanted electrical interference in EEG recordings caused by AC power systems. The most common suppression method, as discussed in [11], is to apply a narrow-band notch filter centered on the supply frequency 50 Hz.

All data are processed with a zero-phase, 2nd-order IIR bi-quadratic (also called biquad) notch centred at $f_0 = \mathbf{50}$ Hz. A quality factor of $Q = \mathbf{25}$ yields a -3 dB stop-band half-width of approximately $f_0/Q \approx 2$ Hz, which suffices to suppress the mains component while preserving nearby SSVEP harmonics. Offline recordings are filtered with a forward–reverse implementation (`filtfilt`) to avoid phase distortion. For real-time streaming the same biquad runs causally, introducing a fixed group delay of four samples ($\approx 16\,\mathrm{ms}$), later compensated in software. The frequency response of the notch can be seen in the appendix A.1

Note on Q-factor. $Q = f_0/\text{bandwidth}$ at the -3 dB points. Higher Q values produce a narrower, deeper notch; lower Q values widen the notch but risk attenuating adjacent frequencies. A value of 25 provides a practical compromise for the 5–45 Hz SSVEP analysis band.

5.3. Artifact Removal

Brain–computer interface (BCI) applications using EEG, such as SSVEP-based systems, must contend with various physiological artifacts that can obscure the true brain signals. In the context of BCIs, the most significant artifacts are those generated by eye activity (blinks or eye movements) and by muscle activity [13]. These artifacts can introduce large spurious EEG fluctuations that distort the genuine neural activity as can be seen in figure 5.1, potentially leading to misinterpretation of user intent. Eye-blink artifacts are typically low-frequency, high-amplitude deflections most pronounced in frontal electrodes, while muscle artifacts (from facial or neck muscles) have a broad frequency spectrum and can occur across many channels. Eye movement and cardiac (ECG) artifacts tend to be more localized and can often be mitigated using reference channels (e.g. EOG electrodes), but muscle (EMG) artifacts are especially challenging to remove due to their high amplitude and widespread, multi-source nature [14]. Robust artifact removal methods are therefore critical to ensure the reliability of EEG-based BCI systems. The focus will be on removing ocular and muscular artifacts using the adaptive filtering

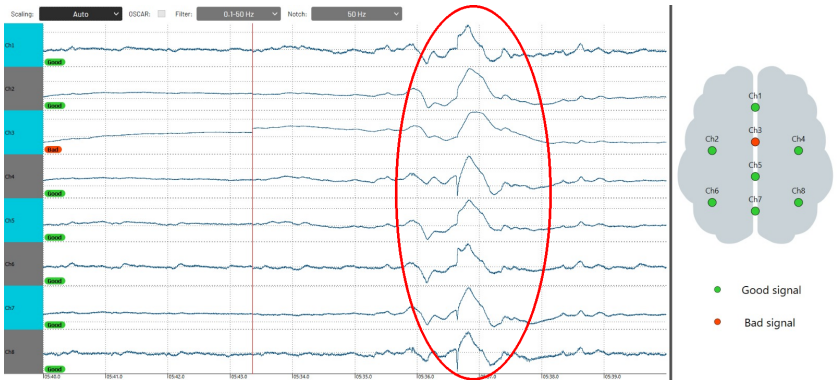

Figure 5.1: Eye blink artifacts

5.3.1. Artifact Removal via Adaptive Filtering

Adaptive filtering is a real-time signal processing technique that can continuously estimate and subtract artifacts from EEG signals [15]. The principle is to treat the artifact removal problem as an adaptive noise cancellation task: one channel (or set of channels) serves as a reference that captures the artifact, and an adaptive filter tries to regress out that artifact from the primary EEG channels. In our setup, we use channel 1 as a reference for eye-blink artifacts, since channel 1 is located near the eye and reliably picks up blink-related EOG activity [16]. Not having dedicated EOG electrodes, channel 1 effectively acts as an EOG channel in this context. Prior to feeding channel 1 into the adaptive filter, we apply a Savitzky–Golay (SG) smoothing filter to it [17]. The Savitzky–Golay filter performs a local polynomial smoothing of the signal, which helps reduce high-frequency EEG and noise while preserving the shape

and peak of the blink artifact. This yields a cleaner reference signal $r(n)$ that predominantly contains the blink artifact to be removed.

In summary, the LMS-based artifact removal as dicussed here [15] treats the blink signal as a regressor that is adaptively scaled and subtracted from each contaminated channel. This approach does not require an explicit calibration (unlike standard regression methods which need a predetermined regression coefficient), because the filter weights automatically adjust to the optimal values over time. The use of a reference channel is of course crucial: the adaptive filter cannot remove artifacts for which it has no reference. Thus, it is effective for artifacts like eye blinks or heartbeats if a reference is provided, but purely internal artifacts like widespread muscle noise are harder to eliminate unless some reference or modeling of them is available. In our SSVEP BCI, we found the LMS filter to be effective in suppressing blink transients in the occipital channels in real time. The adaptive filter quickly zeroed in on the appropriate weight to subtract out each blink, while largely preserving the frequency-specific SSVEP content of the EEG.

The adaptive filter then operates as follows. Let $x(n)$ denote the raw EEG signal from a channel of interest (e.g. an occipital channel used for SSVEP) which is a mixture of the true brain signal $s(n)$ and artifact $a(n)$. This can be modeled as:

$$x(n) = s(n) + a(n) \tag{5.5}$$

where $s(n)$ is the underlying clean EEG (desired signal) and $a(n)$ is the artifact. The reference input $r(n)$ is fed into an adaptive filter (a Finite Impulse Response filter of order M) that produces an output $\hat{a}(n)$, which is the estimator of the artifact in $x(n)$. In a simple configuration, $\hat{a}(n)$ can be a linear combination of the reference signal and its recent samples:

$$\hat{a}(n) = \sum_{k=0}^{M-1} w_k(n)\, r\big(n-k\big) \tag{5.6}$$

where $w_k(n)$ are the adaptive filter weights at time n. Initially, the weights can be zero or small random values. At each time step, the filter output $\hat{a}(n)$ is subtracted from the primary input $x(n)$ to obtain the error (or cleaned signal)

$$e(n) = x(n) - \hat{a}(n). \tag{5.7}$$

This error $e(n)$ is the current estimate of the artifact-free EEG (it contains the residual brain signal plus any remaining artifact). The adaptive algorithm then updates the filter weights $\mathbf{w}(n) = [w_0(n), \ldots, w_{M-1}(n)]^T$ in a manner that minimizes the mean squared error $E[e(n)^2]$. A widely used adaptation rule is the Least Mean Squares (LMS) algorithm, which adjusts the weights in the negative gradient direction of the squared error. The LMS weight update equation is:

$$w_k(n+1) = w_k(n) + \mu\, e(n)\, r\big(n-k\big), \quad k = 0, 1, \ldots, M-1, \tag{5.8}$$

where μ is a small positive step-size (learning rate) controlling the adaptation speed. In vector form,

$$\mathbf{w}(n+1) = \mathbf{w}(n) + \mu\, e(n)\, \mathbf{r}(n), \quad \mathbf{r}(n) = [r(n),\, r(n-1), \ldots, r(n-M+1)]^T. \tag{5.9}$$

By minimizing the error, the algorithm effectively cancels the artifact from $x(n)$, yielding $e(n) \approx s(n)$, the cleaned EEG signal. We note that other adaptation algorithms exist (e.g. Recursive Least Squares, which converges faster at the cost of higher computation), but LMS is attractive for its simplicity and low computational load, making it feasible for real-time use. In fact, adaptive filtering approaches have been demonstrated to be stable, fast-converging, and suitable for on-line removal of EOG artifacts in EEG.

5.4. Summary

Table 5.1 summarises the filter chain applied in the order listed, it delivers a processed EEG stream that is phase-accurate offline and latency-bounded online.

Table 5.1: Digital filters and artefact-removal stage in the preprocessing pipeline

Stage	Method	Order / Length	Cut-offs (Hz)	Q/BW
DC removal	HP Butter.	4	>0.5	—
Band-pass SSVEP	BP Butter.	4	5–45	—
Line noise	Notch biquad	2	50	$Q = 25$
Artifact removal	LMS adaptive filter	5	—	—

Figures 5.2 and 5.3 show a 10-s epoch before and after the full filtering chain.

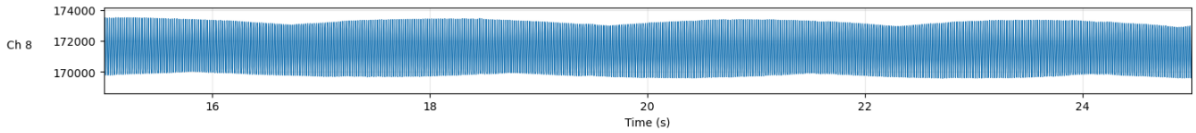

Figure 5.2: Raw EEG: drifting baseline, broadband muscle noise, and a dominant 50 Hz mains peak obscure the SSVEP content.

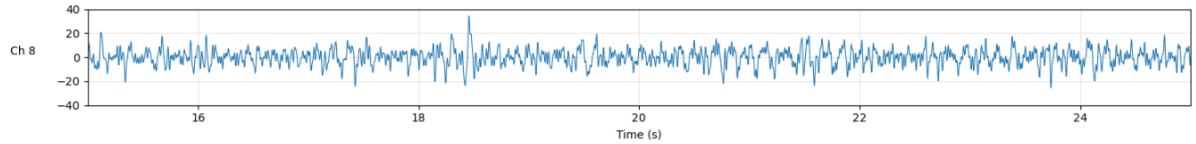

Figure 5.3: Filtered EEG: preprosessing and artifact removal applied.

6

Results

In this chapter, the outcomes of our analyses are presented. First, the signal-to-noise ratios computed in both the time and frequency domains are reported. Then, the spectral integrity of our EEG recordings is assessed via FFT-based validation.

6.1. SNR results

Time Domain SNR Results

Time-domain SNR was computed by comparing the power at each stimulation frequency during flicker against the corresponding frequency's power in baseline recordings. Mean SNR values across subjects and conditions are presented in table 6.1.

Frequency-Domain SNR Results

Frequency-domain SNR was calculated by dividing the power at each target frequency by the average power of its neighboring bins. The distribution of frequency-domain SNR values across participants is shown in table 6.1. This measure emphasizes the presence of the SSVEP peak above the local spectral background.

	Time-SNR		Time-SNR		Freq-SNR		Freq-SNR	
Trial	**lin mean**	**lin std**	**dB mean**	**dB std**	**lin mean**	**lin std**	**dB mean**	**dB std**
1	3.203	2.175	5.056	3.374	1.063	0.083	0.265	−10.794
2	1.882	1.029	2.745	0.123	1.772	1.659	2.485	2.199
3	124.714	124.205	20.959	20.941	1.703	1.406	2.313	1.479
4	1.204	1.110	0.806	0.454	1.050	1.022	0.211	0.096
5	15.864	12.129	12.004	10.838	4.985	2.238	6.976	3.498
6	10.702	9.280	10.294	9.679	4.105	1.265	6.133	1.020
7	3.709	0.846	5.692	−0.730	3.242	1.686	5.108	2.267
8	8.210	3.564	9.144	5.522	8.872	6.726	9.480	8.278
9	4.740	2.195	6.758	3.415	1.896	0.927	2.779	−0.331
10	0.872	0.754	−0.594	−0.473	0.929	0.897	−0.320	−0.473
11	2.642	2.465	4.219	3.918	3.797	3.695	5.794	5.676
12	0.397	0.284	−4.015	−5.462	0.188	0.044	−7.266	−13.560

Table 6.1: Time- and Frequency-Domain SNR from figures 6.1 and 6.2

In Table 6.1, the frequency-domain SNR values line up with the single-trial spectra in Figures 6.1 and 6.2. Ratios above about 2, as in Trials 5 and 8, come with a clear peak at the stimulus frequency. Ratios near or below 1, as in Trials 2, 4, 10, and 12, match spectra that follow a $1/f$ curve and show no peak. Trial 3 exposes a weakness of the time-domain metric; its very high baseline-referenced SNR is driven by a short broadband burst, so the frequency-domain measure still reports only a modest

response. Overall, the frequency-domain SNR gives the clearest view of stimulus-locked activity, while the time-domain SNR mainly flags large power shifts that may be artifacts. Because most trials sit close to the noise floor, we find no significant peaks at the intended stimulation frequencies, and the data lack SSVEP responses strong enough for high-quality classification.

6.2. FFT-Based Signal Validation

To confirm spectral fidelity, the FFT was applied to channel 6, 7 and 8 and the power spectra were examined at stimulus frequencies.

FFT Analysis of Subject Recordings

The frequency-domain plots created by the signal-processing group do not show the strong spectral peaks that should appear at 8.57 Hz or 12 Hz. As seen in Figures 6.1 and 6.2, most power lies at low frequencies and then falls off in a typical $1/f$ pattern. Near the red lines that mark the target frequencies, only small bumps are visible. Their height is about the same as the power in neighbouring bins, so the evoked signal is almost lost in the noise.

Because the target bins are barely higher than the local baseline, the estimated SNR is low. In other words, the brain's response at the flicker frequency is roughly equal to the background EEG fluctuations. The second harmonics at 17.14 Hz and 24 Hz (green dashed lines) behave the same way: no clear peaks appear, which further suggests that the visual stimulus failed to drive a strong steady-state response.

Without sharp spectral lines at the stimulus frequencies, there is no narrowband "signal" towering above the "noise." This makes reliable SSVEP detection difficult. In recordings with high SNR one would expect a pronounced spike that rises several-fold above the baseline. Here, the data show either a very weak response or one that is masked by ongoing activity—possibly the brain's natural alpha rhythm in the 8–12 Hz band. As a result, these trials do not provide SSVEP signals strong enough for dependable analysis or classification.

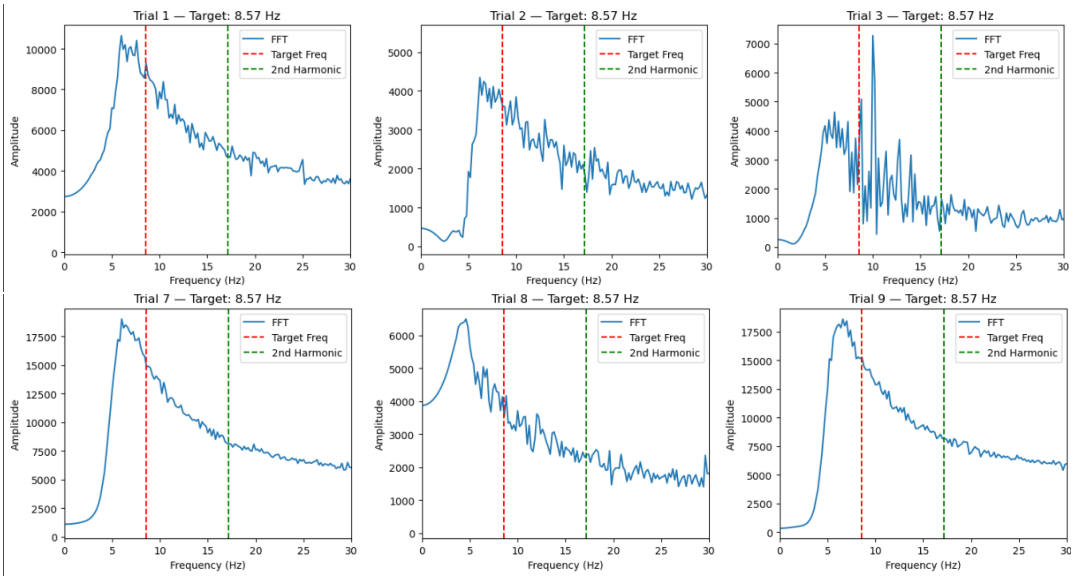

Figure 6.1: FFT of trials with target frequency 8.57 Hz

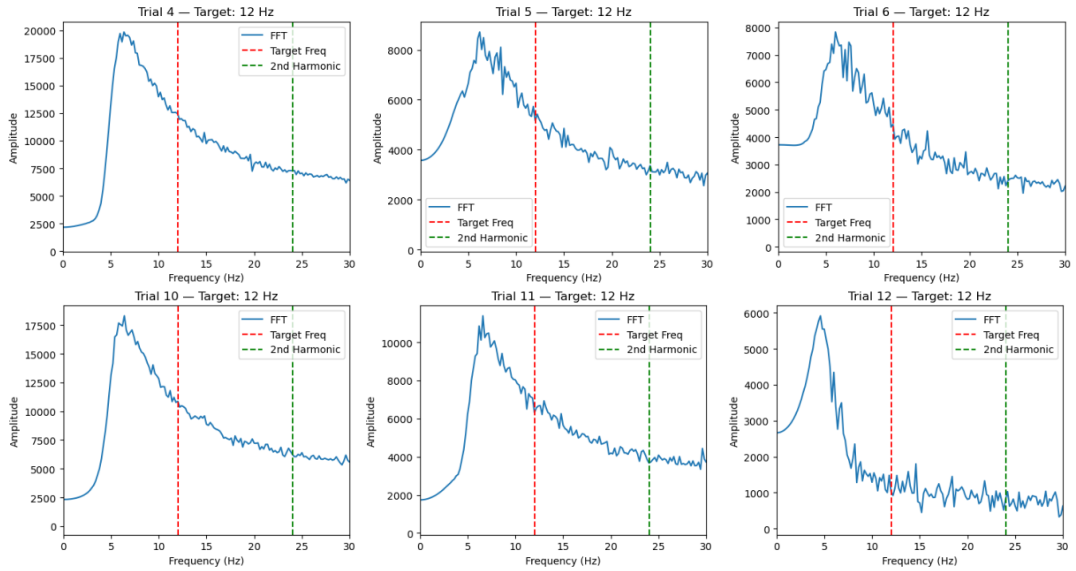

Figure 6.2: FFT of trials with target frequency 12 Hz

FFT analysis of induced sine wave

Figure 6.1 and 6.2 show the FFT across channels 6, 7 and 8 during visual stimulation at 8.57 Hz and 12 Hz. Although past studies have reported clear SSVEP peaks in this range, our recordings did not reveal consistent peaks at the stimulus frequencies. To confirm that this absence of peaks was not due to a flaw in our processing or hardware, we next injected a clean 12 Hz sine wave into the headset via a function generator, this circuit can be found in appendix B.1. As illustrated in Figure 6.3, this produced a sharp, narrowband peak at 10 Hz, demonstrating that our filtering and PSD estimation procedures and the acquisition system itself are capable of resolving periodic signals when presented under controlled conditions.

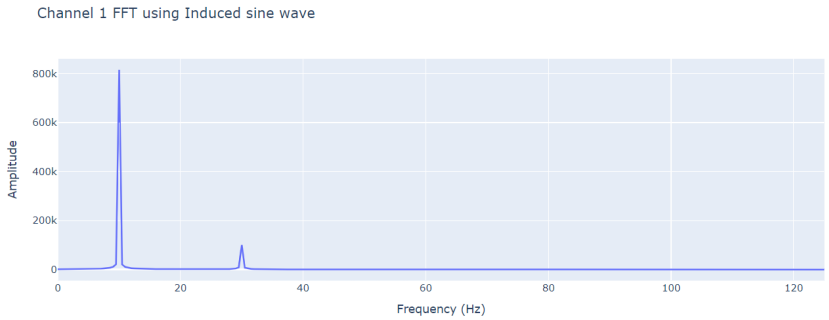

Figure 6.3: induced sine wave FFT at 10 Hz

6.3. Future work

Current blink suppression relies on LMS with channel 1 as a reference. A first improvement is using an EOG electrode (detects pure eyeblinks) [18]. A cleaner reference should speed up convergence and lower residual blink leakage.

The LMS stage itself can grow. A multi-reference adaptive canceller could ingest vertical and horizontal EOG together with a neck-EMG channel. More inputs let the filter tackle saccades and jaw-tension bursts in one pass[19].

ICA already works offline but still needs manual bad-IC pruning. Automatic classifiers such as *ICLabel* [20], *MARA*, or *ADJUST* can take that task over. Integrating one of them or training a small CNN on our own SSVEP data—would remove the bottleneck without heavy runtime costs.

Hybrid pipeline Combine speed and depth:

- LMS (cheap) runs continuously for blinks.
- A sliding-window ICA or SOBI executes every few seconds to remove residual EMG [16].

This staggered scheme keeps latency low while maintaining high overall SNR.

Wavelet or CNN denoisers Wavelet-thresholding can target burst EMG with no reference channels. Recent work [21] shows 1-D U-Nets removing both EOG and EMG in under 10 ms once trained. Evaluating such models on our dataset would test whether deep learning can replace manual parameter tuning.

To conclude, incorporating a dedicated EOG reference and combining ICA with LMS filtering are the next steps for future development of this project.

7

Conclusion

In this report, the development and testing of an EEG data acquisition and preprocessing system for an SSVEP-based Brain-Computer Interface were described. The signal was processed through several filtering steps and cleaned using an adaptive filter based on the LMS algorithm. The system was tested using both flickering visual stimuli and a clean sine wave to check if everything worked as expected.

The filtering methods successfully removed common types of noise, such as baseline drift, electrical interference, and blinking. However, during the tests with real participants, strong SSVEP responses were not consistently seen. In most cases, the expected frequency peaks were missing or too weak to stand out from the background brain activity.

To check whether this was a problem in the system itself, a 12 Hz sine wave was injected directly into the headset. This test did show a clear frequency peak, confirming that the system and signal processing steps were working correctly. It is therefore likely that the problem lies in how the brain responses are triggered or how much noise is present during recording.

Several suggestions have been made for future improvements, such as using better reference signals, combining multiple artifact removal methods, or trying machine learning tools to clean the signal. These steps could help improve the signal quality and make the system more reliable for real-time use in a BCI.

Bibliography

[1] X.-Y. Liu, W.-L. Wang, M. Liu, *et al.*, "Recent applications of eeg-based brain-computer-interface in the medical field," *Military Medical Research*, vol. 12, Mar. 2025. DOI: 10.1186/s40779-025-00598-z.

[2] L. F. Nicolas-Alonso and J. Gomez-Gil, "Brain computer interfaces, a review," *Sensors*, vol. 12, no. 2, pp. 1211–1279, 2012, ISSN: 1424-8220. DOI: 10.3390/s120201211. [Online]. Available: https://www.mdpi.com/1424-8220/12/2/1211.

[3] M. Orban, M. Elsamanty, K. Guo, S. Zhang, and H. Yang, "A review of brain activity and eeg-based brain–computer interfaces for rehabilitation application," *Bioengineering*, vol. 9, no. 12, 2022, ISSN: 2306-5354. DOI: 10.3390/bioengineering9120768. [Online]. Available: https://www.mdpi.com/2306-5354/9/12/768.

[4] G. A. M. Vasiljevic and L. C. de Miranda and, "Brain–computer interface games based on consumer-grade eeg devices: A systematic literature review," *International Journal of Human–Computer Interaction*, vol. 36, no. 2, pp. 105–142, 2020. DOI: 10.1080/10447318.2019.1612213.

[5] F.-B. Vialatte, M. Maurice, J. Dauwels, and A. Cichocki, "Steady-state visually evoked potentials: Focus on essential paradigms and future perspectives," *Progress in Neurobiology*, vol. 90, no. 4, pp. 418–438, 2010, ISSN: 0301-0082. DOI: https://doi.org/10.1016/j.pneurobio.2009.11.005. [Online]. Available: https://www.sciencedirect.com/science/article/pii/S0301008209001853.

[6] E. Netzer, A. Frid, and D. Feldman, "Real-time eeg classification via coresets for bci applications," *Engineering Applications of Artificial Intelligence*, vol. 89, p. 103 455, Mar. 2020. DOI: 10.1016/j.engappai.2019.103455.

[7] S. Saha, K. A. Mamun, K. Ahmed, *et al.*, "Progress in brain computer interface: Challenges and opportunities," *Frontiers in Systems Neuroscience*, vol. Volume 15 - 2021, 2021, ISSN: 1662-5137. DOI: 10.3389/fnsys.2021.578875. [Online]. Available: https://www.frontiersin.org/journals/systems-neuroscience/articles/10.3389/fnsys.2021.578875.

[8] X. Duart, E. Quiles, F. Suay, N. Chio, E. García, and F. Morant, "Evaluating the effect of stimuli color and frequency on ssvep," *Sensors*, vol. 21, no. 1, p. 117, 2020.

[9] M.-Y. Wang and Z. Yuan, "Eeg decoding of dynamic facial expressions of emotion: Evidence from ssvep and causal cortical network dynamics," *Neuroscience*, vol. 459, pp. 50–58, 2021.

[10] S. R. Schultz, "Signal-to-noise ratio in neuroscience," *Scholarpedia*, vol. 2, no. 6, p. 2046, 2007, revision #137197. DOI: 10.4249/scholarpedia.2046.

[11] A. Delorme, "Eeg is better left alone," *Scientific reports*, vol. 13, no. 1, p. 2372, 2023.

[12] V. J. Kartsch, V. P. Kumaravel, S. Benatti, *et al.*, "Efficient low-frequency ssvep detection with wearable eeg using normalized canonical correlation analysis," *Sensors*, vol. 22, no. 24, p. 9803, 2022.

[13] E. J. McDermott, P. Raggam, S. Kirsch, P. Belardinelli, U. Ziemann, and C. Zrenner, "Artifacts in eeg-based bci therapies: Friend or foe?" *Sensors*, vol. 22, no. 1, p. 96, 2021.

[14] S. S. Khan, J. S. Sudan, A. Pathak, R. Pandit, P. Rane, and A. K. Kumawat, "A review of eeg artifact removal methods for brain-computer interface applications," *Ingenierie des Systemes d'Information*, vol. 29, no. 1, p. 247, 2024.

[15] X. Jiang, G.-B. Bian, and Z. Tian, "Removal of artifacts from eeg signals: A review," *Sensors*, vol. 19, no. 5, p. 987, 2019.

[16] B. Hua, "Improved adaptive filtering based artifact removal from eeg signals," in *2020 13th International Congress on Image and Signal Processing, BioMedical Engineering and Informatics (CISP-BMEI)*, IEEE, 2020, pp. 424–428.

[17] F. Abd Rahman and M. Othman, “Real time eye blink artifacts removal in electroencephalogram using savitzky-golay referenced adaptive filtering,” in *International conference for innovation in biomedical engineering and life sciences*, Springer, 2015, pp. 68–71.

[18] S. Puthusserypady and T. Ratnarajah, “H/sup/spl infin//adaptive filters for eye blink artifact minimization from electroencephalogram,” *IEEE signal processing letters*, vol. 12, no. 12, pp. 816–819, 2005.

[19] X. Gao, S. Zhang, K. Liu, *et al.*, “An adaptive joint cca-ica method for ocular artifact removal and its application to emotion classification,” *Journal of Neuroscience Methods*, vol. 390, p. 109 841, 2023.

[20] L. Pion-Tonachini, K. Kreutz-Delgado, and S. Makeig, “Iclabel: An automated electroencephalographic independent component classifier, dataset, and website,” *NeuroImage*, vol. 198, pp. 181–197, 2019.

[21] C.-H. Chuang, K.-Y. Chang, C.-S. Huang, and T.-P. Jung, “Ic-u-net: A u-net-based denoising autoencoder using mixtures of independent components for automatic eeg artifact removal,” *NeuroImage*, vol. 263, p. 119 586, 2022.

A

Plots

A.1. Frequency responses

A.1.1. Notch

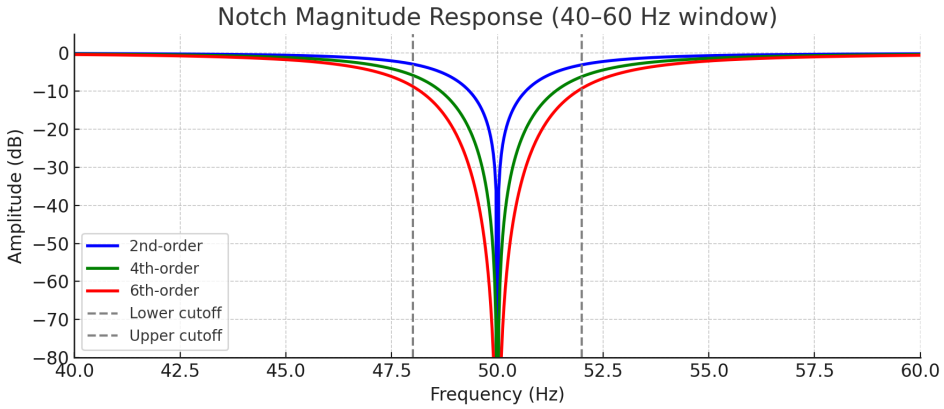

Figure A.1: Frequency response of Butterworth bandstop filter from 48 Hz to 52 Hz. Different orders are compared

A.1.2. Bandpass

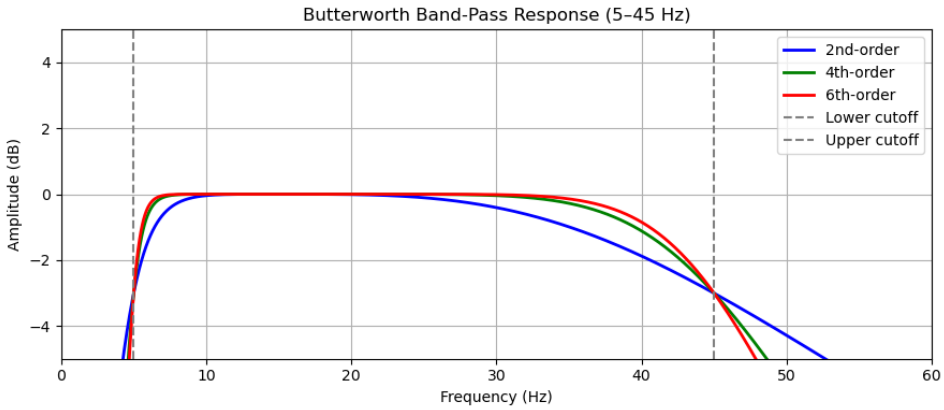

Figure A.2: Frequency response of Butterworth bandpass filter from 5 Hz to 45 Hz. Different orders are compared.

B

Circuit

B.1. Function generator circuit

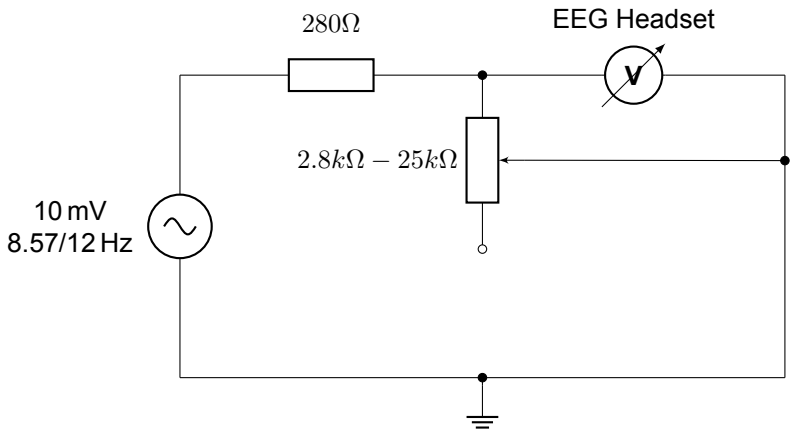

Figure B.1: Measurement setup with function generator and tuneable voltage divider

C

Statement of AI

In the preparation of this Bachelor thesis, AI was used to support code debugging and clarification, correct grammar, and enhance the overall readability of the text. AI was used solely as a supportive tool, and all the content, analysis, and conclusions are the result of our own work. All AI-assisted outputs were carefully reviewed and edited to ensure alignment with academic standards and personal intent.